K^+K^+ scattering length from lattice QCD

Silas R. Beane,[1] Thomas C. Luu,[2] Kostas Orginos,[3,4] Assumpta Parreño,[5] Martin J. Savage,[6] Aaron Torok,[1] and André Walker-Loud[7]

(NPLQCD Collaboration)

[1]*Department of Physics, University of New Hampshire, Durham, New Hampshire 03824-3568, USA*
[2]*N Division, Lawrence Livermore National Laboratory, Livermore, California 94551, USA*
[3]*Department of Physics, College of William and Mary, Williamsburg, Virginia 23187-8795, USA*
[4]*Jefferson Laboratory, 12000 Jefferson Avenue, Newport News, Virginia 23606, USA*
[5]*Departament d'Estructura i Constituents de la Matèria and Institut de Ciències del Cosmos, Universitat de Barcelona, E–08028 Barcelona, Spain*
[6]*Department of Physics, University of Washington, Seattle, Washington 98195-1560, USA*
[7]*Department of Physics, University of Maryland, College Park, Maryland 20742-4111, USA*
(Received 29 October 2007; published 21 May 2008)

The K^+K^+ scattering length is calculated in fully-dynamical lattice QCD with domain-wall valence quarks on the MILC asqtad-improved gauge configurations with rooted-staggered sea quarks. Three-flavor mixed-action chiral perturbation theory at next-to-leading order, which includes the leading effects of the finite lattice spacing, is used to extrapolate the results of the lattice calculation to the physical value of m_{K^+}/f_{K^+}. We find $m_{K^+}a_{K^+K^+} = -0.352 \pm 0.016$, where the statistical and systematic errors have been combined in quadrature.

DOI: 10.1103/PhysRevD.77.094507 PACS numbers: 11.15.Ha, 12.39.Fe

I. INTRODUCTION

Strange hadrons may play a crucial role in the properties and evolution of nuclear material under extreme conditions [1]. The interior of neutron stars provide one such environment in which the densities are high enough that it may be energetically favorable to have strange baryons present in significant quantities, depending upon their interactions with nonstrange hadrons. Further, it may be the case that a kaon condensate forms due to strong interactions between kaons and nucleons [2]. Unfortunately, the theoretical analysis of both scenarios is somewhat plagued by the limited knowledge of the interactions of strange hadrons with themselves and with nonstrange hadrons.

Heavy-ion collisions, such as those at the BNL relativistic heavy-ion collider, also produce nuclear material in an extreme condition. Recent observations suggesting the formation of a low-viscosity fluid are quite exciting as they provide a first glimpse of matter not seen previously. The late-time evolution of such a collision requires an understanding of the interaction between many species of hadrons, not just those of the initial state, including the interactions between strange mesons and baryons. While pion interferometry in heavy-ion collisions is a well-established tool for studying the collision region (for recent theoretical progress, see Refs. [3–5]), the STAR collaboration has recently published the first observation of neutral kaon (K^0_s) interferometry [6]. In the analysis of K^0_s-K^0_s interferometry, the nonresonant contributions to the final state interactions between the kaons were estimated using three-flavor $(SU(3)_L \otimes SU(3)_R)$ chiral perturbation theory (χ-PT), the low-energy effective field theory of QCD. Given the sometimes poor convergence of $SU(3)_L \otimes SU(3)_R$ χ-PT due to the relatively-large kaon mass compared to the scale of chiral symmetry breaking ($\Lambda_\chi \sim 1$ GeV), particularly in the baryon sector, it is important to be able to verify that the nonresonant contributions to KK scattering are indeed small, as estimated in χ-PT.

In this work we present the first lattice QCD calculation of the K^+K^+ scattering length. The calculations are performed on the coarse MILC lattices (with a preliminary calculation on one ensemble of the fine MILC lattices) and three-flavor mixed-action χ-PT (MAχ-PT), which includes the leading-order lattice-spacing effects, is used to extrapolate to the continuum and to the (isospin-symmetric) physical value of the meson masses. We find that at the physical value of m_{K^+}/f_{K^+}

$$m_{K^+}a_{K^+K^+} = -0.352 \pm 0.016, \tag{1}$$

where the statistical and systematic errors have been combined in quadrature.

The π, K, and η are identified as the pseudo-Goldstone bosons associated with the spontaneous breaking of the approximate chiral symmetry of quantum chromodynamics (QCD), and therefore the form of their interactions is highly constrained. In fact, at leading order in χ-PT, the scattering of two of these mesons is uniquely determined [7]. Corrections to the leading order scattering amplitude arise in a systematic expansion about the chiral limit [8,9],

scaling generically as $(m^2_{\pi,K,\eta}/\Lambda^2_\chi)^n$ where n counts the order in the chiral expansion [10]. For obvious reasons, $SU(3)$ χ-PT is expected to converge more slowly than two-flavor χ-PT.

There is a wealth of phenomenological and theoretical knowledge concerning low-energy $\pi\pi$ scattering. The chiral extrapolation formulas for $\pi\pi$ scattering are known to two loops, or next-to-next-to-leading order (NNLO), in both $SU(2)$ [11,12] and $SU(3)$ [13] χ-PT. Combined with a Roy equation analysis [14–16], this has allowed for remarkably-precise determinations of the two s-wave $\pi\pi$ scattering lengths [17–19]. In the case of the $K\pi$ systems, the extrapolation formulas for the scattering amplitudes are known to one [20–22] and two loops [23] and have allowed for theoretical predictions of the $I = 1/2$ and $I = 3/2$ scattering lengths. However, the uncertainty in these theoretical predictions is substantial. There are proposed experiments to study the $K\pi$ atoms by the DIRAC collaboration [24] at CERN, J-PARC, and GSI, which will significantly reduce the uncertainty in these scattering lengths. To date, there have been no experimental determinations of the $I = 1$ KK scattering length, $a^{I=1}_{KK}$, but recently it has been calculated at next-to-leading order (NLO) in χ-PT [25].

The methods for studying two-particle interactions in a finite Euclidean volume are well-known [26–29]. The interaction energy of two hadrons in a finite volume uniquely determines $p\cot\delta(p)$, and hence their scattering amplitude, below kinematic thresholds. The scattering parameters, such as the scattering length and effective range, can then be determined from calculations of $p\cot\delta(p)$ over a range of energies. These methods paved the way for pioneering quenched QCD calculations of two-particle interactions a little over a decade ago [30–34]. Since then, there have been a number of additional quenched calculations of the $I = 2$ $\pi\pi$ scattering length [35–42]. The first dynamical calculation of $\pi\pi$ interactions (including the phase shift) was performed by the CP-PACS collaboration with two flavors ($n_f = 2$) of improved Wilson fermions [43] and pion masses in the range $500 \lesssim m_\pi \lesssim 1100$ MeV. Recently, dynamical calculations of the $I = 2$ $\pi\pi$ scattering length with three flavors of light quarks ($n_f = 2 + 1$) were performed with pion masses in the range $300 \lesssim m_\pi \lesssim 500$ MeV. These calculations used a mixed-action scheme of domain-wall valence fermions on asqtad-improved staggered sea fermions at a single lattice spacing of $b \sim 0.125$ fm [44,45], and used mixed-action χ-PT (MAχ-PT) (which describes the finite-lattice-spacing effects) calculations of the scattering length [46] to extrapolate to the physical meson masses. Only recently has the first calculation of the $I = 3/2$ $K\pi$ scattering length in quenched QCD been performed [47], and a fully-dynamical $n_f = 2 + 1$ calculation [48] followed shortly afterward. When combined with χ-PT, this latter calculation allowed for a simultaneous prediction of the $I = 1/2$ and $I = 3/2$ $K\pi$ scattering lengths using the NLO extrapolation formulas [48].

This paper is organized as follows. Section II contains the details of our mixed-action lattice QCD calculation. Discussion of the relevant correlation functions and an outline of the methodology and fitting procedures can also be found in this section. The results of the lattice calculation and the analysis with MAχ-PT are presented in Sec. III. In this section, the various sources of systematic uncertainty are identified and quantified. In Sec. IV we conclude.

II. METHODOLOGY AND DETAILS OF THE LATTICE CALCULATION

The computation in this paper uses the mixed-action lattice QCD scheme developed by LHPC [49,50]. Domain-wall fermion propagators were generated from a smeared source on $n_f = 2 + 1$ asqtad-improved [51,52] coarse configurations generated with rooted-staggered sea quarks [53]. Hypercubic-smeared [54–57] gauge links were used in the domain-wall fermion action to improve chiral symmetry (further details about the mixed-action scheme can be found in Refs. [48,58]). The mixed-action calculations we have performed involved computing the valence-quark propagators using the domain-wall formulation of lattice fermions, on each gauge-field configuration of an ensemble of the MILC lattices that are generated using the staggered formulation of lattice fermions [59–63] and taking the fourth root of the fermion determinant, i.e. domain-wall valence quarks on a rooted-staggered sea. In the continuum limit the $n_f = 2$ staggered action has an $SU(8)_L \otimes SU(8)_R \otimes U(1)_V$ chiral symmetry due to the four-fold taste degeneracy of each flavor, and each pion has 15 degenerate additional partners. At finite lattice spacing this symmetry is broken and the taste multiplets are no longer degenerate, but have splittings that are $\mathcal{O}(\alpha^2 b^2)$. While there is no proof, there are arguments to suggest that taking the fourth root of the fermion determinant recovers the contribution from a single Dirac fermion.[1] The results of this paper assume that the fourth-root trick recovers the correct continuum limit of QCD.

The present calculations were performed predominantly with the coarse MILC lattices with a lattice spacing of $b \sim 0.125$ fm, and a spatial extent of $L \sim 2.5$ fm. On these configurations, the strange quark was held fixed near its physical value while the degenerate light quarks were varied over a range of masses; see Table I and Refs. [58,78–81] for details. Further, preliminary calculations were performed on 506 configurations of one fine MILC ensemble. On the coarse MILC lattices, Dirichlet

[1]For a nice introduction to staggered fermions and the fourth-root trick, see Ref. [64]. For the most recent discussions regarding the continuum limit of staggered fermions with the fourth-root trick, see Refs. [57,65–77].

TABLE I. The parameters of the MILC gauge configurations and domain-wall propagators used in this work. The subscript l denotes light quark (up and down), and s denotes the strange quark. The superscript dwf denotes the bare-quark mass for the domain-wall fermion propagator calculation. The last column is the number of configurations times the number of sources per configuration.

Ensemble	bm_l	bm_s	bm_l^{dwf}	bm_s^{dwf}	$10^3 \times bm_{\rm res}$ [a]	# of propagators
2064f21b676m007m050	0.007	0.050	0.0081	0.081	1.604	468×16
2064f21b676m010m050	0.010	0.050	0.0138	0.081	1.552	658×20
2064f21b679m020m050	0.020	0.050	0.0313	0.081	1.239	486×24
2064f21b681m030m050	0.030	0.050	0.0478	0.081	0.982	564×8
2896f2b709m0062m031	0.0062	0.031	0.0080	0.0423	~ 0.25 [b]	506×1

[a]Computed by the LHP collaboration.
[b]Estimated on a small number of configurations.

boundary conditions were implemented to reduce the original time extent of 64 down to 32 and thus save a factor of 2 in computational time.[2] While this procedure leads to minimal degradation of a nucleon signal, it does limit the number of time slices available for fitting meson properties. By contrast, on the fine MILC ensemble, antiperiodic boundary conditions were implemented and all time slices are available.

When determining the mass of the valence quarks there is an ambiguity due to the nondegeneracy of the 16 staggered bosons associated with each pion. One could choose to match to the taste-singlet meson or to any of the mesons that become degenerate in the continuum limit. Given that $I = 1$ KK scattering length has been calculated at NLO in χ-PT, PQχ-PT, and MAχ-PT (which, by definition, includes the leading finite lattice-spacing effects) in Ref. [25],[3] the effects of matching can be described, and removed, by calculations appropriate to the choice of matching [83] (provided the meson masses remain in the chiral regime). The choice of tuning to the lightest taste of staggered meson mass, as opposed to one of the other tastes, provides for the "most chiral" domain-wall mesons and therefore reduces the error in extrapolating to the physical point. The mass splitting between the domain-wall mesons and the staggered taste-identity mesons, which characterizes the unitarity violations present in the calculation, is then given by [84,85]

$$b^2 m_{\pi_l}^2 - b^2 m_{\pi_{dwf}}^2 \simeq b^2 \Delta_{\rm I} = 0.0769(22)(\text{l.u.}) \quad \text{coarse;}$$
$$= 0.0295(27)(\text{l.u.}) \quad \text{fine,} \qquad (2)$$

where l.u. denotes lattice units.

[2]On the Tungsten machine at NCSA, running on 32 dual xeon nodes (64 processors) it takes approximately 80 minutes to generate one light quark domain-wall propagator (with $l_s = 16$) yielding $m_\pi \sim 290$ MeV.

[3]The PQχ-PT and MAχ-PT expressions for the $I = 1$ KK scattering length are identical in form at NLO. This is not unique to this quantity and can be understood on more general grounds, as mixed-action theories with chirally-symmetric valence fermions exhibit many universal features [82].

A summary of the lattice parameters and resources used in this work is given in Table I. In order to generate large statistics on the existing MILC configurations, multiple propagators from sources displaced both temporally and spatially on the lattice were computed. The correlators were blocked so that one average correlator per configuration was used in the subsequent jackknife statistical analysis.

In order to determine the interaction energy between the two kaons, both the single-kaon, $C_{K^+}(t)$, and two-kaon, $C_{K^+K^+}(p, t)$, correlation functions were computed, where t is the Euclidean time separation between the hadronic source and sink operators and p denotes the magnitude of the equal and opposite spatial momentum of each kaon. The single-kaon correlation function is

$$C_{K^+}(t) = \sum_{\mathbf{x}} \langle K^-(t, \mathbf{x}) K^+(0, \mathbf{0}) \rangle, \qquad (3)$$

where the sum over all spatial sites projects onto the zero-momentum state, $\mathbf{p} = 0$. A correlation function which projects onto the K^+K^+ s-wave state in the continuum limit is

$$C_{K^+K^+}(p, t) = \sum_{|\mathbf{p}|=p} \sum_{\mathbf{x},\mathbf{y}} e^{i\mathbf{p}\cdot(\mathbf{x}-\mathbf{y})} \langle K^-(t, \mathbf{x}) K^-(t, \mathbf{y}) K^+(0, \mathbf{0}) K^+(0, \mathbf{0}) \rangle. \qquad (4)$$

In Eqs. (3) and (4), $K^+(t, \mathbf{x}) = \bar{s}(t, \mathbf{x}) \gamma_5 u(t, \mathbf{x})$ is a Gaussian-smeared interpolating field for the charged kaon. In the relatively-large spatial volumes used in the calculation, the interaction energy between the two kaons is a small fraction of the total energy, which is dominated by the kaon masses. To determine this energy, the ratio of correlation functions,

$$G_{K^+K^+}(p, t) \equiv \frac{C_{K^+K^+}(p, t)}{C_{K^+}(t) C_{K^+}(t)} \rightarrow \sum_{n=0}^{\infty} \mathcal{A}_n e^{-\Delta E_n t}, \qquad (5)$$

was constructed, with the arrow denoting the large-time, infinite-number-of-gauge-configurations limit (far from the boundary). Because of the periodic boundary conditions imposed on the propagators computed on the fine

lattices, the K^+ correlation function becomes a single cosh function far from the source, while the K^+K^+ correlation function becomes the sum of two cosh's, one depending upon m_{K^+} and the other depending upon $E_{K^+K^+}$, leading to a nontrivial form for $G_{K^+K^+}(p,t)$. As an alternative method to calculating the interaction energy (and a check of the systematics), a jackknife analysis of the difference between the energies extracted from the long-time behavior of the double- and single-kaon correlation functions individually was performed, finding results in agreement with those determined from Eq. (5). The interaction energy is related to the two-particle energy eigenvalues and twice the kaon mass,

$$\Delta E_n \equiv E_n^{KK} - 2m_K = 2\sqrt{p_n^2 + m_K^2} - 2m_K. \tag{6}$$

In the absence of interactions, the energy levels occur at values of the momenta $\mathbf{p} = 2\pi\mathbf{j}/L$ where $\mathbf{j}$ is an integer triplet, corresponding to the allowed single-particle momentum modes in a cubic volume. In the interacting theory, the two-particle eigenmomenta, p_n, are shifted from these values and can be determined from Eq. (6) and the calculated interaction energy. The Lüscher formula [26–29] can then be used to determine the infinite-volume scattering parameters from the real part of the inverse scattering amplitude by solving the equation

$$p\cot\delta(p) = \frac{1}{\pi L}\mathbf{S}\left(\frac{pL}{2\pi}\right), \tag{7}$$

which is valid below the inelastic threshold. The regulated three-dimensional sum is [86]

$$\mathbf{S}(\eta) \equiv \sum_{\mathbf{j}}^{|\mathbf{j}|<\Lambda} \frac{1}{|\mathbf{j}|^2 - \eta^2} - 4\pi\Lambda, \tag{8}$$

which runs over all triplets of integers $\mathbf{j}$ such that $|\mathbf{j}| < \Lambda$ and the limit $\Lambda \to \infty$ is implicit. The scattering parameters are then related to $p\cot\delta(p)$ through the effective-range expansion

$$p\cot\delta(p) = \frac{1}{a} + \frac{1}{2}rp^2 + \mathcal{O}(p^4), \tag{9}$$

where a is the scattering length and r is the effective range. For naturally-sized scattering lengths and small interaction momenta, $p\cot\delta(p)$ is predominantly given by the inverse scattering length.

III. ANALYSIS AND THE CHIRAL AND CONTINUUM EXTRAPOLATIONS

In order to extract quantities of interest from the calculated correlation function, the argument of a single exponential function must be determined, along with its uncertainty. This can be accomplished in several ways, and we have chosen to analyze effective mass and scattering length plots. For instance, the effective energy splitting of two kaons in the lattice volume is constructed from the two-kaon correlation function via

$$\Delta E_{K^+K^+}(t) = \log\left(\frac{G_{K^+K^+}(0,t)}{G_{K^+K^+}(0,t+1)}\right). \tag{10}$$

The uncertainty associated with $\Delta E_{K^+K^+}(t)$ on each time slice is determined by the jacknife procedure. To construct the effective scattering length, $a_{K^+K^+}(t)$, the energy $\Delta E(t)$ is inserted into Eq. (7) to yield a scattering length at each time slice and its uncertainty. To remove any scale-setting ambiguities, the scattering length is multiplied by the "effective" kaon mass, $m_K(t)$. The effective scattering length plots associated with each lattice ensemble are shown in Fig. 2. There is no unique method with which to extract the quantity of interest from the effective mass or scattering length plots, which receive contributions from an infinite number of exponentials. For lattices with an infinite time extent the correlation functions will be dominated by a single exponential function dictated by the lowest energy state, and hence the effective mass scattering length plot will tend to a constant. In the asymptotically large-time region, a fit is performed to extract the quantity of interest. For any real lattice calculation, the time extent is not infinitely large, and so a fitting region must be decided upon that allows for the optimal determination of the quantity of interest from the calculation. On the coarse lattices with the Dirichlet boundary, there are exponentially decaying contributions from the source, and exponentially growing contributions from the boundary, and the "signal region" is in the middle. The actual fitting region is dictated by a region over which the effective mass or scattering length plots are time independent within their uncertainties. Clearly, determining the fitting interval is somewhat subjective as deviations from constant behavior are implicitly assumed to result from large energy gaps in the spectrum in the finite volume. On the coarse lattices, single exponential behavior of the kaon mass correlation function is seen to set in beyond time slice $t = 6$, and remain until $t \sim 16$, as seen in Fig. 1. Once a fitting range has been chosen, a correlated χ^2/dof fit is performed to extract the quantity of interest, with its statistical uncertainty determined by the range for which $\chi^2 \to \chi^2 + 1$, in the usual way. However, there is a systematic error associated with each quantity due to the fact that the fitting range is not uniquely defined. We estimate the fitting systematic uncertainty by the range of values obtained by varying the fitting intervals at either end, and by removing one or more time slices at random and refitting. In the third panel of Fig. 1, corresponding to the kaon mass for $m_\pi \sim 490$ MeV, it is clear that fitting to a constant kaon mass over the interval between $t = 9$ and $t = 15$ yields an unappealingly large χ^2/dof due to the small statistical uncertainties at each time slice. The absolute variation is at the $\sim$1% level. Clearly one could choose another fitting interval and obtain a different kaon mass at

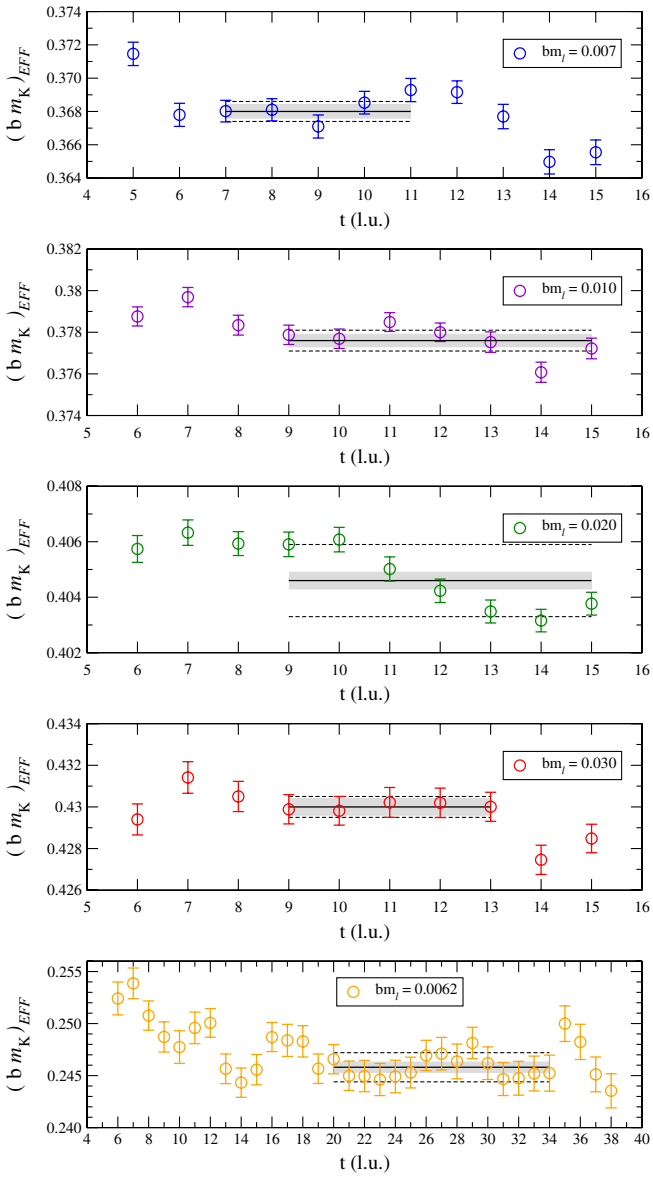

FIG. 1 (color online). The effective $m_{K^+}(t)$ plots. The solid black lines and shaded regions are fits with 1-σ statistical uncertainties (Table II). The dashed lines correspond to the statistical and systematic (Table II) uncertainties added in quadrature.

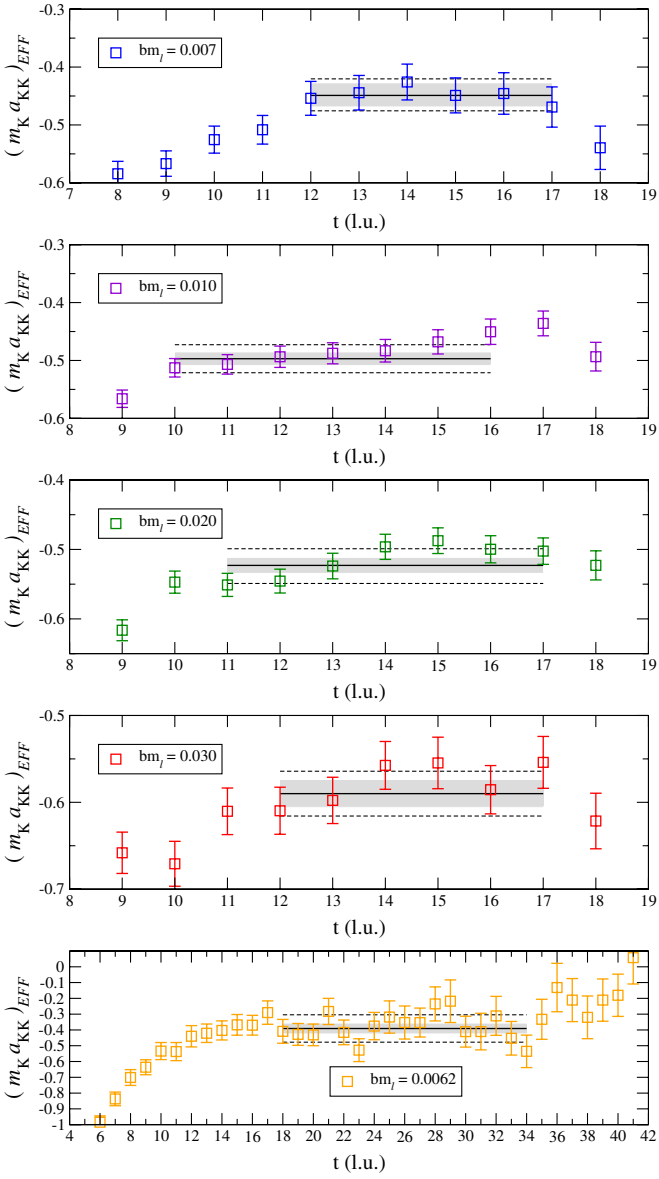

FIG. 2 (color online). The effective K^+K^+ scattering length times the effective m_{K^+} as a function of time slice. The solid black lines and shaded regions are fits with 1-σ statistical uncertainties (Table II). The dashed lines correspond to the statistical and systematic (Table II) uncertainties added in quadrature.

the $\sim$1% level, and it is clear that the total uncertainty will be dominated by the systematic fitting uncertainty. Therefore, the fitting intervals, central values, and statistical errors should be viewed as representative and it is the total error that imparts the information that is extracted from the data. The statistical error and central values by themselves provide only an incomplete discussion of the calculation. One could use a fitting interval from $t = 6$ to $t = 9$ and obtain a value that, with the systematic error that we have determined, would be an equally valid result to present.

The statistical errors are determined from a jackknife analysis, while the quoted systematic errors are estimated from both the range of fits as well as the two methods of determining the interaction energy described in Sec. II. In Table II the calculated values of the meson masses, decay constants, two-particle energy shifts, and scattering lengths are presented. Effective kaon mass plots and effective scattering length plots are shown in Figs. 1 and 2, respectively.

A. Mixed-action χ-PT at one loop

The lattice QCD calculations performed in this work are isospin symmetric, $m_u = m_d$, and do not include electromagnetism. Therefore isospin is a good quantum number. Having computed the K^+K^+ scattering length at a number

TABLE II. Masses, energies, and scattering lengths determined from the lattice calculation. The first uncertainty assigned to each quantity is statistical, determined with the jackknife procedure, and the second uncertainty is an estimated fitting systematic.

Quantity	$m_l = 0.007$	$m_l = 0.010$	$m_l = 0.020$	$m_l = 0.030$	$m_l = 0.0062$
bm_π	0.1846(4)(2)	0.2226(4)(3)	0.3104(3)(15)	0.3747(4)(8)	0.1453(5)(13)
Fit Range	8–14	9–13	9–15	6–13	17–39
bm_K	0.3680(4)(4)	0.3776(3)(4)	0.4046(3)(13)	0.4300(4)(3)	0.2458(5)(13)
Fit Range	7–11	9–15	9–15	9–13	20–34
m_π/f_K	1.712(4)(3)	2.069(3)(5)	2.835(3)(11)	3.335(4)(9)	1.978(15)(12)
m_K/f_K	3.412(5)(4)	3.509(3)(6)	3.695(3)(10)	3.827(4)(9)	3.344(19)(21)
ΔE_{KK}(l.u.)	0.006 19(30)(32)	0.006 63(15)(35)	0.006 06(14)(22)	0.006 13(19)(10)	0.004 37(36)(105)
Fit Range	12–17	10–16	11–17	12–17	18–34
$m_{K^+}a_{K^+K^+}$ $(b \neq 0)$	−0.448(19)(20)	−0.497(10)(22)	−0.523(10)(23)	−0.590(15)(21)	−0.391(28)(82)

of unphysical pion masses and at a finite-lattice-spacing, isospin-symmetric MAχ-PT is used to extrapolate to the physical (isospin-symmetric) meson masses and to the continuum.

In Ref. [25], the expression for the $I = 1KK$ scattering length was determined to NLO in χ-PT, including corrections due to mixed-action lattice artifacts. As with the $I = 2\ \pi\pi$ scattering length [46], it was demonstrated that when the mixed-action extrapolation formula is expressed in terms of the lattice-physical parameters computed on the lattice,[4] m_π, m_K, and f_K, there are no lattice-spacing-dependent counterterms at $\mathcal{O}(b^2)$, $\mathcal{O}(b^2 m_K^2)$, or $\mathcal{O}(b^4)$. There are finite-lattice-spacing-dependent corrections, proportional to $b^2\Delta_{\rm I}$, and therefore entirely determined to this order in MAχ-PT. Again, as with the $I = 2\ \pi\pi$ system, the NLO mixed action (MA) formula for $m_K a_{KK}^{I=1}$ does not depend upon the mixed valence-sea meson masses, and therefore does not require knowledge of the mixed-meson masses [87]. This allows for a precise determination of the predicted MA corrections to the scattering length. At NLO in MAχ-PT, the scattering length takes the form

$$\begin{aligned} m_K a_{KK}^{I=1}(b \neq 0) &= -\frac{m_K^2}{8\pi f_K^2}\Bigg\{1 + \frac{m_K^2}{(4\pi f_K)^2}\Bigg[C_\pi \ln\left(\frac{m_\pi^2}{\mu^2}\right) \\ &\quad + C_K \ln\left(\frac{m_K^2}{\mu^2}\right) + C_X \ln\left(\frac{\tilde{m}_X^2}{\mu^2}\right) + C_{ss} \ln\left(\frac{m_{ss}^2}{\mu^2}\right) \\ &\quad + C_0 - 32(4\pi)^2 L_{KK}^{I=1}(\mu)\Bigg]\Bigg\}, \end{aligned} \tag{11}$$

where the various coefficients, C_i, along with $\tilde{m}_X^2$ and m_{ss}^2, can be found in Appendix E of Ref. [25]. To account for the predicted MA corrections, one can either use Eq. (11) to directly fit the results of the lattice calculation (Table II) or one can determine the quantity

$$\Delta_{\rm MA}(m_K a_{KK}^{I=1}) = m_K a_{KK}^{I=1}|_{\rm MA} - m_K a_{KK}^{I=1}|_{\chi{\rm PT}}, \tag{12}$$

collected in Tables III and IV, subtract this from the results of the lattice calculation and use the NLO χ-PT expression for the scattering length,

$$\begin{aligned} m_K a_{KK}^{I=1} &= -\frac{m_K^2}{8\pi f_K^2}\Bigg\{1 + \frac{m_K^2}{(4\pi f_K)^2}\Bigg[2\ln\left(\frac{m_K^2}{\mu^2}\right) \\ &\quad - \frac{2m_\pi^2}{3(m_\eta^2 - m_\pi^2)}\ln\left(\frac{m_\pi^2}{\mu^2}\right) + \frac{2(20m_K^2 - 11m_\pi^2)}{27(m_\eta^2 - m_\pi^2)} \\ &\quad \times \ln\left(\frac{m_\eta^2}{\mu^2}\right) - \frac{14}{9} - 32(4\pi)^2 L_{KK}^{I=1}(\mu)\Bigg]\Bigg\}. \end{aligned} \tag{13}$$

As there is only one counterterm at NLO, it can be determined on each ensemble. In order to carry out this analysis, further sources of systematic errors are identified; higher-order effects in the chiral expansion, $\Delta_{\rm NNLO}(m_K a_{KK}^{I=1})$; exponentially-suppressed finite-volume effects, $\Delta_{\rm FV}(m_K a_{KK}^{I=1})$; residual chiral symmetry breaking effects from the domain-wall action, $\Delta_{m_{\rm res}}(m_K a_{KK}^{I=1})$; and the error in truncating the effective-range expansion with the inverse scattering length, $\Delta_{\rm range}(m_K a_{KK}^{I=1})$. These various sources of systematic uncertainty, as well as the predicted mixed-action corrections, the adjusted scattering lengths, and the determined values of $L_{KK}^{I=1}(\mu)$ are given in Tables III and IV. In the following sections, each source of systematic uncertainty is addressed in turn.

1. NNLO χ-PT corrections

The NNLO extrapolation formula for $m_K a_{KK}^{I=1}$ does not exist, and therefore estimates of contributions from higher order in the chiral expansion are limited to power-counting arguments. A conservative estimate is provided by

$$\Delta_{\rm NNLO}(m_K a_{KK}^{I=1}) = \pm\frac{2\pi m_K^6}{(4\pi f_K)^6}\left[\ln\left(\frac{m_K^2}{f_K^2}\right)\right]^2, \tag{14}$$

and the resulting uncertainties are given in Tables III and IV.

[4] Quantities calculated directly from the correlation functions are denoted as lattice-physical parameters. These are not extrapolated to the continuum, to infinite volume nor to the physical quark mass point.

TABLE III. The continuum limit of the scattering length at the physical point on the coarse MILC lattices, the extracted counterterm that enters at NLO in χ-PT, and the various systematic uncertainties that have been identified beyond those associated with fitting. The correction factors, Δ_i, are defined in the text. The first uncertainty associated with each scattering length is statistical, the second is the systematic uncertainty from Table II, and the third is from the systematic uncertainties presented in this table (combined in quadrature). The first uncertainty associated with each $L_{KK}^{I=1}(\mu = f_K)$ is statistical, while the second is systematic (all systematics combined in quadrature).

Quantity	$m_l = 0.007$	$m_l = 0.010$	$m_l = 0.020$	$m_l = 0.030$
$\Delta_{\rm MA}(m_K a_{KK}^{I=1})$	$-0.0067(14)$	$-0.0062(16)$	$-0.0052(19)$	$-0.0048(21)$
$\Delta_{\rm NNLO}(m_K a_{KK}^{I=1})$	± 0.016	± 0.019	± 0.028	± 0.037
$\Delta_{\rm FV}(m_K a_{KK}^{I=1})$	± 0.001	± 0.001	± 0.000	± 0.000
$\Delta_{m_{\rm res}}(m_K a_{KK}^{I=1})$	± 0.007	± 0.006	± 0.005	± 0.004
$\Delta_{\rm range}(m_K a_{KK}^{I=1})$	± 0.008	± 0.008	± 0.008	± 0.007
$m_{K^+} a_{K^+K^+}$ $(b \to 0)$	$-0.441(19)(20)(19)$	$-0.491(10)(22)(22)$	$-0.518(10)(23)(30)$	$-0.585(15)(21)(38)$
$32(4\pi)^2 L_{KK}^{I=1}(f_K)$	7.3(5)(8)	6.8(3)(8)	7.7(2)(8)	7.4(3)(8)

2. Finite-volume effects in mixed-action χ-PT

Lüscher's relation between the two-particle energy levels in a finite volume and their infinite-volume scattering parameters receives exponential corrections which depend upon the lattice size and the lightest particle in the spectrum, and generically scale as $e^{-m_\pi L}$. In Ref. [88], the exponential volume corrections were determined for the $I = 2$ $\pi\pi$ system. Using these methods, one can also determine the exponential volume corrections for the mixed-action K^+K^+ system. These exponentially-suppressed volume corrections are formally subleading compared to the effective-range corrections which have not been included, and provide an estimate of the finite-volume corrections. These terms are denoted as

$$\Delta_{\rm FV}(m_K a_{KK}^{I=1}) = \pm(m_K a_{KK}^{I=1}|_{\rm FV} - m_K a_{KK}^{I=1}|_{\infty V}) \qquad (15)$$

and are collected in Tables III and IV.

TABLE IV. The continuum limit of the scattering length at the physical point on the fine MILC lattices, the extracted counterterm that enters at NLO in χ-PT, and the various systematic uncertainties that have been identified beyond those associated with fitting. The correction factors and uncertainties are discussed in the caption of Table III.

Quantity	$m_l = 0.0062$
$\Delta_{\rm MA}(m_K a_{KK}^{I=1})$	$-0.0048(15)$
$\Delta_{\rm NNLO}(m_K a_{KK}^{I=1})$	± 0.013
$\Delta_{\rm FV}(m_K a_{KK}^{I=1})$	± 0.001
$\Delta_{m_{\rm res}}(m_K a_{KK}^{I=1})$	± 0.004
$\Delta_{\rm range}(m_K a_{KK}^{I=1})$	± 0.004
$m_{K^+} a_{K^+K^+}$ $(b \to 0)$	$-0.387(28)(82)(14)$
$32(4\pi)^2 L_{KK}^{I=1}(f_K)$	8.4(9)(2.6)

3. Residual chiral symmetry breaking

The NLO mixed-action formula, Eq. (11), as well as the corrections of Tables III and IV, were derived assuming valence fermions with perfect chiral symmetry. However, domain-wall fermions are necessarily implemented with a finite fifth dimension which induces residual chiral symmetry breaking. The leading contributions from this residual chiral symmetry breaking can be parametrized with a residual quark mass [61,62],

$$m_l^{dwf} \to m_l^{dwf} + m_{\rm res}, \qquad m_s^{dwf} \to m_s^{dwf} + m_{\rm res}. \qquad (16)$$

However, by expressing the MAχ-PT formula in terms of the lattice-physical meson masses, the dominant contribution from these $m_{\rm res}$ terms are automatically included. This leaves corrections at NLO (assuming $m_{\rm res} \sim m_q$ in the expansion), some of which have undetermined coefficients. Naive dimensional analysis [89] can be used to estimate the size of these terms,

$$\Delta_{m_{\rm res}}(m_K a_{KK}^{I=1}) = \pm \frac{8\pi m_K^4}{(4\pi f_K)^4} \frac{m_{\rm res}}{m_l}, \qquad (17)$$

which are shown in Tables III and IV.

4. Range corrections

When the spatial dimensions of the lattice are large compared to the range of the interaction, and the scattering length is of natural size, as is the case for K^+K^+ scattering at the quark masses used in this work, the effective range first enters at $\mathcal{O}(L^{-6})$ in the expansion of the two-hadron energy in powers of $1/L$. Therefore, neglecting the effective-range parameter introduces a $\sim$0.2% uncertainty in the extracted values of $m_{K^+} a_{K^+K^+}$, assuming $r \sim 1/(2m_\pi)$ for $m_\pi \ll m_K$. To be conservative, a 1% systematic uncertainty due to the neglect of the effective range is assigned to the scattering length determined on each ensemble.

TABLE V. The results of fitting three-flavor MAχ-PT at NLO to the computed scattering lengths, as described in the text. The values of $m_{K^+}a_{K^+K^+}$ are those extrapolated to the physical (isospin-symmetric) meson masses and to the continuum. The first uncertainty is statistical and the second is systematic (as described in the text).

FIT	$32(4\pi)^2 L_{KK}^{I=1}(f_K)$	$m_{K^+}a_{K^+K^+}$ (extrapolated)	χ^2/dof
A	7.3(1)(4)	$-0.347 \pm 0.003 \pm 0.009$	0.22
B	7.3(2)(5)	$-0.347 \pm 0.004 \pm 0.011$	0.32
C	6.9(2)(6)	$-0.355 \pm 0.005 \pm 0.013$	0.14

B. Extrapolation to the physical point

Calculations on the four coarse lattice ensembles yield pion and kaon masses of approximately $(m_\pi, m_K) \sim$ (290, 580), (350, 595), (490, 640) and (590 ,675) MeV. The chiral expansion will converge better for smaller meson masses, and one method to examine the convergence of the chiral expansion is to selectively "prune" the heaviest data sets [44,45,48]. This is done by first determining $L_{KK}^{I=1}(\mu = f_K)$ by fitting to all four data points (fit A), then removing the heaviest point and fitting (fit B), and finally removing the heaviest two points and fitting (fit C). The results of these fits are collected in Table V. The extracted values of $L_{KK}^{I=1}$ from each of the fits are consistent with each other within the uncertainties. In analogy with the comparison convention employed for $\pi^+\pi^+$, the lattice data is extrapolated to the physical values of $m_{\pi^+}/f_{K^+} = 0.8731 \pm 0.0096$, $m_{K^+}/f_{K^+} = 3.088 \pm 0.018$, and $m_\eta/f_{K^+} = 3.425 \pm 0.0019$ assuming isospin symmetry, and the absence of electromagnetism. Taking the range of values of $L_{KK}^{I=1}$ spanned by these fits, we find

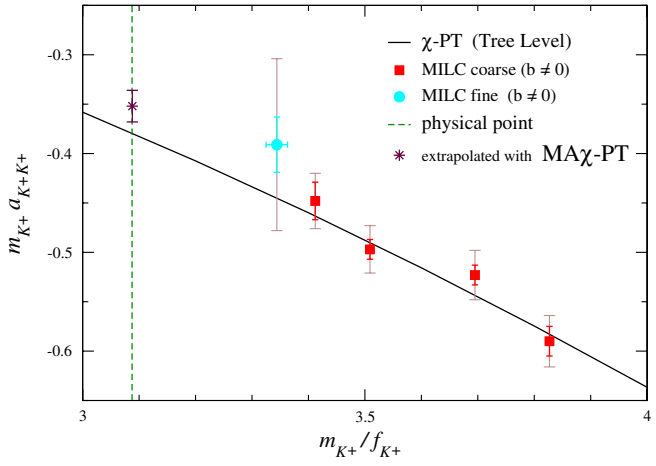

FIG. 3 (color online). $m_{K^+}a_{K^+K^+}$ versus m_{K^+}/f_{K^+}. The points with error bars are the results of this lattice calculation (not extrapolated to the continuum) on both the coarse and fine MILC lattices. The solid curve corresponds to the tree-level prediction of χ-PT, and the point denoted by a star and its associated uncertainty is the value extrapolated to the physical meson masses and to the continuum. The smaller uncertainty associated with each point is statistical, while the larger uncertainty is the statistical and fitting systematic combined in quadrature.

$$\begin{aligned} m_{K^+}a_{K^+K^+} &= -0.352 \pm 0.016, \\ 32(4\pi)^2 L_{KK}^{I=1}(\mu = f_K) &= 7.1 \pm 0.7, \end{aligned} \tag{18}$$

where the statistical and systematic errors have been combined in quadrature. The results are shown in Fig. 3. It is somewhat surprising that the calculated scattering lengths are consistent, within uncertainties, with tree-level χ-PT. This was also found to be the case for $\pi^+\pi^+$ scattering even at large pion masses.

C. Comparing K^+K^+ scattering with $\pi^+\pi^+$ scattering

A comparison between the lattice calculations of $\pi^+\pi^+$ [45] and K^+K^+ scattering lengths allows for a study of flavor-$SU(3)$ breaking in the scattering amplitude due to terms that are beyond NLO in χ-PT. The linear combination of Gasser-Leutwyler coefficients contributing to the $I = 2\,\pi\pi$ scattering length at NLO is the same as the combination contributing to the $I = 1\,KK$ scattering length [25]

$$L_{KK}^{I=1}(\mu) = L_{\pi\pi}^{I=2}(\mu). \tag{19}$$

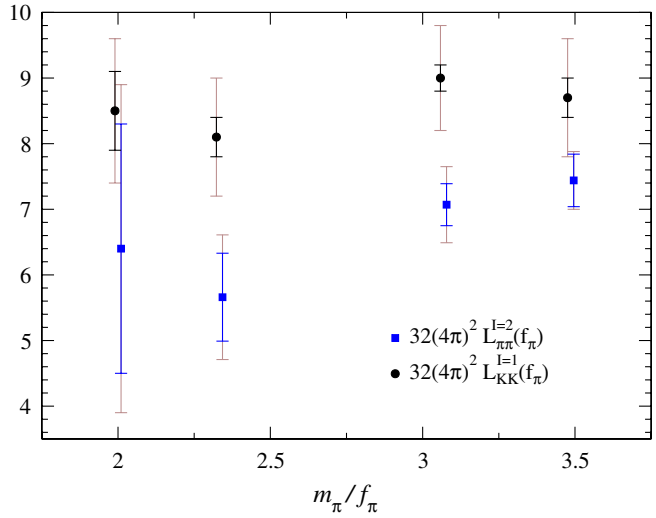

FIG. 4 (color online). $32(4\pi)^2 L_{KK}^{I=1}(f_\pi)$ (circles) and $32(4\pi)^2 L_{\pi\pi}^{I=2}(f_\pi)$ (squares) versus m_π/f_π. The sets have been slightly displaced horizontally for convenience of viewing. The smaller uncertainty associated with each point is statistical, while the larger uncertainty is the statistical and fitting systematic combined in quadrature.

To compare extractions of these counterterms, the scales at which they are evaluated must be the same, and the scale-dependence of $L_{KK}^{I=1}(\mu)$ is

$$32(4\pi)^2 L_{KK}^{I=1}(\mu) = 32(4\pi)^2 L_{KK}^{I=1}(\mu_0) - \frac{28}{9}\ln\left(\frac{\mu^2}{\mu_0^2}\right). \quad (20)$$

The counterterms extracted from the mixed-action lattice calculations are shown in Fig. 4 as a function of m_π/f_π. It is clear that while there appears to be a difference between $L_{KK}^{I=1}(f_\pi)$ and $L_{\pi\pi}^{I=2}(f_\pi)$, more precise calculations of both scattering lengths, particularly at the lightest pion masses, are required for further exploration of higher-order terms in the chiral expansion.

IV. DISCUSSION

We have presented results of a lattice QCD calculation of the K^+K^+ scattering length performed with domain-wall valence quarks on asqtad-improved MILC configurations with $2+1$ dynamical staggered quarks. The calculations were performed on the coarse MILC lattices with a lattice spacing of $b \sim 0.125$ fm (with a preliminary calculation on one ensemble of the fine MILC lattices with $b \sim 0.09$ fm) and at a single lattice spatial size of $L \sim 2.5$ fm. One-loop MAχ-PT with three flavors of light quarks was used to perform the chiral and continuum extrapolations. Our prediction for the physical value of the K^+K^+ scattering length is $m_{K^+}a_{K^+K^+} = -0.352 \pm 0.016$, and we emphasize once again that this result rests on the assumption that the fourth-root trick recovers the correct continuum limit of QCD. Deviations from Weinberg's tree-level prediction are found to be surprisingly small, consistent with the lattice calculations of the $\pi^+\pi^+$ scattering length at heavier pion masses.

The lowest quark mass at which we have computed the K^+K^+ scattering length corresponds to $m_\pi \sim 290$ MeV. This is determined by the lattices that have been generated by the MILC collaboration, which ultimately is dictated by the amount of computer power available to the USQCD lattice effort. In the near future, lattices will become available at quark masses closer to the physical values, and if the computer power allocated to us increases enough, we will compute the K^+K^+ scattering length at these lighter pion masses. Of course, as one goes to lighter quark mass at fixed lattice spacing, the extent of the fifth dimension of the domain-wall propagator will need to be increased to maintain a suitably small residual mass, further increasing the required computer time, beyond the naive increase with quark mass. As an example, we estimate that it will require 6 times the amount of computer power to compute with $m_\pi \sim 250$ MeV ($l_s = 48$) than with $m_\pi \sim 290$ MeV ($l_s = 16$) for comparable statistics on the coarse lattices, an amount that currently exceeds our allocation from USQCD by approximately a factor of 2.

ACKNOWLEDGMENTS

We thank R. Edwards and B. Joo for help with the QDP + +/Chroma programming environment [90] with which the calculations discussed here were performed. The computations for this work were performed at the Jefferson Lab, Fermilab, Lawrence Livermore National Laboratory, National Center for Supercomputing Applications, and Centro Nacional de Supercomputación (Barcelona, Spain). We are indebted to the MILC and the LHP collaborations for use of their configurations and propagators, respectively. The work of M. J. S. was supported in part by the U.S. Department of Energy under Grant No. DE-FG03-97ER4014. The work of K. O. was supported in part by the U.S. Department of Energy contract No. DE-AC05-06OR23177 (JSA) and by the Jeffress Memorial Trust, Grant No. J-813. The work of A. W. L. was supported in part by the U.S. Department of Energy Grant No. DE-FG02-93ER-40762. The work of S. R. B. and A. T. was supported in part by the National Science Foundation CAREER Grant No. PHY-0645570. Part of this work was performed under the auspices of the U.S. Department of Energy by the University of California, Lawrence Livermore National Laboratory under Contract No. W-7405-Eng-48. The work of A. P. was partly supported by the European Union Contract No. FLAVIAnet MRTN-CT-2006-035482, by the Contract No. FIS2005-03142 from MEC (Spain) and FEDER, and by the Generalitat de Catalunya Contract No. 2005SGR-00343.

[1] D. Page and S. Reddy, Annu. Rev. Nucl. Part. Sci. **56**, 327 (2006).
[2] D. B. Kaplan and A. E. Nelson, Phys. Lett. B **175**, 57 (1986).
[3] J. G. Cramer, G. A. Miller, J. M. S. Wu, and J. H. S. Yoon, Phys. Rev. Lett. **94**, 102302 (2005).
[4] G. A. Miller and J. G. Cramer, J. Phys. G **34**, 703 (2007).
[5] G. A. Miller and J. G. Cramer, Nucl. Phys. **A782**, 251 (2007).
[6] B. I. Abelev *et al.* (STAR Collaboration), Phys. Rev. C **74**, 054902 (2006).
[7] S. Weinberg, Phys. Rev. Lett. **17**, 616 (1966).
[8] S. Weinberg, Physica (Amsterdam) **96A**, 327 (1979).
[9] J. Gasser and H. Leutwyler, Ann. Phys. (N.Y.) **158**, 142 (1984).
[10] J. Gasser and H. Leutwyler, Nucl. Phys. **B250**, 465 (1985).
[11] J. Bijnens, G. Colangelo, G. Ecker, J. Gasser, and M. E. Sainio, Phys. Lett. B **374**, 210 (1996).

[12] J. Bijnens, G. Colangelo, G. Ecker, J. Gasser, and M. E. Sainio, Nucl. Phys. **B508**, 263 (1997); **B517**, 639(E) (1998).

[13] J. Bijnens, P. Dhonte, and P. Talavera, J. High Energy Phys. 01 (2004) 050.

[14] S. M. Roy, Phys. Lett. **36B**, 353 (1971).

[15] J. L. Basdevant, C. D. Froggatt, and J. L. Petersen, Nucl. Phys. **B72**, 413 (1974).

[16] B. Ananthanarayan, G. Colangelo, J. Gasser, and H. Leutwyler, Phys. Rep. **353**, 207 (2001).

[17] G. Colangelo, J. Gasser, and H. Leutwyler, Nucl. Phys. **B603**, 125 (2001).

[18] I. Caprini, G. Colangelo, and H. Leutwyler, Int. J. Mod. Phys. A **21**, 954 (2006).

[19] H. Leutwyler, arXiv:hep-ph/0612112.

[20] V. Bernard, N. Kaiser, and U. G. Meißner, Nucl. Phys. **B357**, 129 (1991).

[21] V. Bernard, N. Kaiser, and U. G. Meißner, Phys. Rev. D **43**, 2757 (1991).

[22] B. Kubis and U. G. Meißner, Phys. Lett. B **529**, 69 (2002).

[23] J. Bijnens, P. Dhonte, and P. Talavera, J. High Energy Phys. 05 (2004) 036.

[24] http://dirac.web.cern.ch/DIRAC/future.html.

[25] J. W. Chen, D. O'Connell, and A. Walker-Loud, Phys. Rev. D **75**, 054501 (2007).

[26] K. Huang and C. N. Yang, Phys. Rev. **105**, 767 (1957).

[27] H. W. Hamber, E. Marinari, G. Parisi, and C. Rebbi, Nucl. Phys. **B225**, 475 (1983).

[28] M. Lüscher, Commun. Math. Phys. **105**, 153 (1986).

[29] M. Lüscher, Nucl. Phys. **B354**, 531 (1991).

[30] S. R. Sharpe, R. Gupta, and G. W. Kilcup, Nucl. Phys. **B383**, 309 (1992).

[31] R. Gupta, A. Patel, and S. R. Sharpe, Phys. Rev. D **48**, 388 (1993).

[32] Y. Kuramashi, M. Fukugita, H. Mino, M. Okawa, and A. Ukawa, Phys. Rev. Lett. **71**, 2387 (1993).

[33] Y. Kuramashi, M. Fukugita, H. Mino, M. Okawa, and A. Ukawa, arXiv:hep-lat/9312016.

[34] M. Fukugita, Y. Kuramashi, M. Okawa, H. Mino, and A. Ukawa, Phys. Rev. D **52**, 3003 (1995).

[35] H. R. Fiebig, K. Rabitsch, H. Markum, and A. Mihaly, Few-Body Syst. **29**, 95 (2000).

[36] C. a. Liu, J. h. Zhang, Y. Chen, and J. P. Ma, arXiv:hep-lat/0109010.

[37] C. Liu, J. h. Zhang, Y. Chen, and J. P. Ma, Nucl. Phys. **B624**, 360 (2002).

[38] S. Aoki *et al.* (JLQCD Collaboration), Phys. Rev. D **66**, 077501 (2002).

[39] S. Aoki *et al.* (CP-PACS Collaboration), Phys. Rev. D **67**, 014502 (2003).

[40] K. J. Juge (BGR Collaboration), Nucl. Phys. B, Proc. Suppl. **129**, 194 (2004).

[41] S. Aoki *et al.* (CP-PACS Collaboration), Phys. Rev. D **71**, 094504 (2005).

[42] X. Li *et al.* (CLQCD Collaboration), J. High Energy Phys. 06 (2007) 053.

[43] T. Yamazaki *et al.* (CP-PACS Collaboration), Phys. Rev. D **70**, 074513 (2004).

[44] S. R. Beane, P. F. Bedaque, K. Orginos, and M. J. Savage, Phys. Rev. D **73**, 054503 (2006).

[45] S. R. Beane, T. C. Luu, K. Orginos, A. Parreño, M. J. Savage, A. Torok, and A. Walker-Loud (NPLQCD Collaboration), Phys. Rev. D **77**, 014505 (2008).

[46] J. W. Chen, D. O'Connell, R. S. Van de Water, and A. Walker-Loud, Phys. Rev. D **73**, 074510 (2006).

[47] C. Miao, X. i. Du, G. w. Meng, and C. Liu, Phys. Lett. B **595**, 400 (2004).

[48] S. R. Beane, P. F. Bedaque, T. C. Luu, K. Orginos, E. Pallante, A. Parreño, and M. J. Savage, Phys. Rev. D **74**, 114503 (2006).

[49] D. B. Renner *et al.*, Nucl. Phys. B, Proc. Suppl. **140**, 255 (2005).

[50] R. G. Edwards *et al.*, Proc. Sci., LAT2005 (2005) 056.

[51] K. Orginos, D. Toussaint, and R. L. Sugar, Phys. Rev. D **60**, 054503 (1999).

[52] K. Orginos and D. Toussaint, Phys. Rev. D **59**, 014501 (1998).

[53] C. W. Bernard *et al.*, Phys. Rev. D **64**, 054506 (2001).

[54] A. Hasenfratz and F. Knechtli, Phys. Rev. D **64**, 034504 (2001).

[55] T. A. DeGrand, A. Hasenfratz, and T. G. Kovacs, Phys. Rev. D **67**, 054501 (2003).

[56] T. A. DeGrand, Phys. Rev. D **69**, 014504 (2004).

[57] S. Dürr, C. Hoelbling, and U. Wenger, Phys. Rev. D **70**, 094502 (2004).

[58] S. R. Beane, P. F. Bedaque, T. C. Luu, K. Orginos, E. Pallante, A. Parreño, and M. J. Savage (NPLQCD Collaboration), Nucl. Phys. **A794**, 62 (2007).

[59] D. B. Kaplan, Phys. Lett. B **288**, 342 (1992).

[60] Y. Shamir, Phys. Lett. B **305**, 357 (1993).

[61] Y. Shamir, Nucl. Phys. **B406**, 90 (1993).

[62] V. Furman and Y. Shamir, Nucl. Phys. **B439**, 54 (1995).

[63] Y. Shamir, Phys. Rev. D **59**, 054506 (1999).

[64] *Lattice Methods for Quantum Chromodynamics*, edited by Thomas DeGrand and Carleton DeTar (World Scientific, Singapore, 2006), ISBN 981-256-727-5.

[65] M. Creutz, arXiv:hep-lat/0603020.

[66] C. Bernard, Phys. Rev. D **73**, 114503 (2006).

[67] C. Bernard, M. Golterman, Y. Shamir, and S. R. Sharpe, Phys. Lett. B **649**, 235 (2007).

[68] M. Creutz, Phys. Lett. B **649**, 241 (2007).

[69] C. Bernard, M. Golterman, and Y. Shamir, Phys. Rev. D **73**, 114511 (2006).

[70] C. Bernard, M. Golterman, and Y. Shamir, Proc. Sci., LAT2006 (2006) 205 [arXiv:hep-lat/0610003].

[71] M. Creutz, Phys. Lett. B **649**, 230 (2007).

[72] M. Creutz, Phys. Lett. B **649**, 241 (2007).

[73] S. Dürr and C. Hoelbling, Phys. Rev. D **71**, 054501 (2005).

[74] S. Dürr and C. Hoelbling, Phys. Rev. D **74**, 014513 (2006).

[75] A. Hasenfratz and R. Hoffmann, Phys. Rev. D **74**, 014511 (2006).

[76] Y. Shamir, Phys. Rev. D **75**, 054503 (2007).

[77] S. R. Sharpe, Proc. Sci., LAT2006 (2006) 022 [arXiv:hep-lat/0610094].

[78] S. R. Beane, P. F. Bedaque, K. Orginos, and M. J. Savage, Phys. Rev. Lett. **97**, 012001 (2006).

[79] S. R. Beane, K. Orginos, and M. J. Savage, Phys. Lett. B **654**, 20 (2007).

[80] S. R. Beane, K. Orginos, and M. J. Savage, Nucl. Phys. **B768**, 38 (2007).

[81] S. R. Beane, P. F. Bedaque, K. Orginos, and M. J. Savage, Phys. Rev. D **75**, 094501 (2007).

[82] J. W. Chen, D. O'Connell, and A. Walker-Loud, arXiv: 0706.0035.
[83] O. Bar, C. Bernard, G. Rupak, and N. Shoresh, Phys. Rev. D **72**, 054502 (2005).
[84] C. Aubin *et al.* (MILC Collaboration), Phys. Rev. D **70**, 114501 (2004).
[85] C. Bernard *et al.* (MILC Collaboration), Proc. Sci., LAT2006 (2006) 163 [arXiv:hep-lat/0609053].
[86] S. R. Beane, P. F. Bedaque, A. Parreño, and M. J. Savage, Phys. Lett. B **585**, 106 (2004).
[87] K. Orginos and A. Walker-Loud, arXiv:0705.0572.
[88] P. F. Bedaque, I. Sato, and A. Walker-Loud, Phys. Rev. D **73**, 074501 (2006).
[89] A. Manohar and H. Georgi, Nucl. Phys. **B234**, 189 (1984).
[90] R. G. Edwards and B. Joo (SciDAC Collaboration), Nucl. Phys. B, Proc. Suppl. **140**, 832 (2005).